DOI: 10.15276/aait.01.2021.4
UDC 621.314.5

DYNAMIC PERFORMANCES OF THE SHUNT ACTIVE POWER FILTER CONTROL SYSTEM

Sergiy M. Peresada[1)]
ORCID: 0000-0001-8948-722X; sergei.peresada@gmail.com
Sergiy M. Kovbasa[1)]
ORCID: 0000-0002-2954-455X; skovbasa@ukr.net
Yuriy M. Zaichenko[1)]
ORCID: 0000-0002-2933-7737; zaychenko_yura@i.ua
[1)] National Technical University of Ukraine “Igor Sikorsky Kyiv Polytechnic Institute”, 37, Peremogy Ave., Kyiv, Ukraine

ABSTRACT

Harmonic pollution of the electrical mains is well known and well-studied phenomena. Active power filter being a powerful tool to meet the requirements of regulatory documents regulating the electricity quality. Despite this fact, practical implementation of the active power filter is still connected with significant difficulties. In particular, existing systems typically use fast Fourier transform methods or instantaneous power theory to estimate the harmonic composition of the mains current. However, the use of fast Fourier transform requires high computing power of the control system, and the implementation of the theory of instantaneous power significantly increases the requirements for the power part of the active filter. The application of another approach - selective compensation of harmonics, makes it possible to reduce computational requirements and significantly simplify the technical implementation of the active filter and at the same time to achieve an acceptable level of distortion compensation. In this paper, the shunt active power filter control system is designed and investigated. Proposed control system consist of selective harmonics observer, feedback-linearizing current controller, dc-link controller and mains voltage observer. Harmonics observer is tuned according to simplified approach, provides selective estimation of the load current harmonics and produce the compensation current reference for the current controller. Nonlinear dc-link voltage controller guarantees decoupled from current compensation process asymptotic regulation of the average dc-link voltage. Mains voltage vector adaptive observer provides magnitude, angular position and frequency estimation. Proposed control system is implemented on digital signal processor TMS320F28335 end verified experimentally. Results of experimental investigations together with results of simulations confirm effectiveness of proposed solution. Developed control system can be used for shunt active filters implementation.

Keywords: Shunt active power filter; dc-link voltage controller; harmonic distortions; selective harmonic compensation

For citation: **Peresada S. M., Kovbasa S. M., Zaichenko Y. M. Dynamic Performances of the Shunt Active Power Filter Control System. *Applied Aspects of Information Technology.* 2021; Vol.4 No.1: 47–56. DOI: 10.15276/aait.01.2021.4**

INTRODUCTION

Fast increasing quantity of non-linear electrical consumers in modern electricals grids leads to significant current harmonic distortions which has negative influence on grid equipment and different electronic devices. In order to resolve this problem the policy of limitations on permissible level of current distortion is applied [1]. In order to meet power quality standards final customer should be use special power filters, passive or active. The traditional passive filters have well known significant limitations for higher harmonics compensation [2] and therefore starting from 1990-th the active power filters are considered as more preferable tool for power quality improvement. A great number of publications and researches are devoted to this problem [3-4], [5-6], [7]. Among all configurations of active power filters a wide prevalence have shunt active power filters (SAF), designed for current harmonics and reactive power compensation, Fig. 1.

From the control point of view, there are three main SAF control tasks: high order current harmonics estimation in order to obtain compensation current reference; compensation current control loops design in order to provide proper injection of the compensation current into distorted mains; SAF dc-link voltage control in order to maintain SAF stability and possibility to generate compensation current.

1. LITERATURE OVERVIEW

Despite a presence of numerous commercial active power filters, their design is still characterized as a complex and expensive task, because high performance SAF operation requires high computation power, high-quality power electronics and measurement devices. In order to reduce these requirements, simplify design process and total SAF cost the approach of selective harmonic compensation is proposed [8-9]. Due to this approach only the most critical current harmonics should be estimated and compensated. After such compensation mains current waveform may have still non-ideal sinusoidal shape, but requirements of the power quality standard will be fulfilled. As it is shown in [10-11], [12] the most critical harmonics are 5th, 7th, 11th, 13th, 17th, 19th and have to be compensated in selective mode.

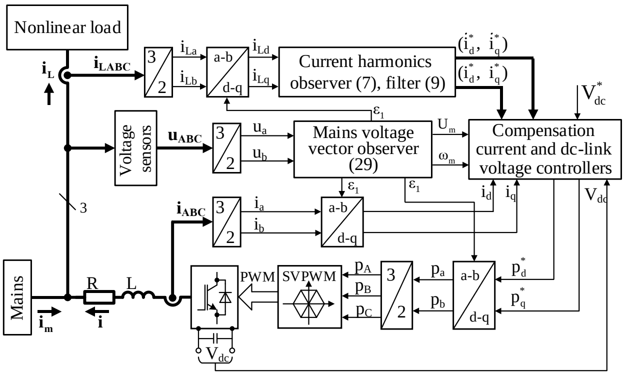

Fig. 1. **Functional diagram of the shunt active filter**
***Source*: compiled by the author**

In order to provide selective detection of current harmonics the most widespread approaches are: implementation of Band-Pass filters and Discrete Fourier transformation in stationary reference frame or in synchronous reference frame oriented by line voltage vector, multiple rotating reference frame approach [13].

A problem of the current control loop design for compensation current generation is not widely described in the present literature. In most cases hysteresis controllers [14] or simple "high-gain" PI current controllers [15-16], utilized for compensation current reference tracking. An approach for multi-loop current tracking improvement is presented in [17].

Important key point of SAF operation is keeping the dc-link voltage in the admissible range in order to avoid SAF instability. In general case, the dc-link voltage control is provided by means of independent voltage control loop with linear PI-controller [18]. But such approach does not provide full decoupling of current tracking and dc-link voltage control, because the derivative of dc-link voltage regulation current component is unknown and could not be compensated in current controllers. Implementation of the approach presented in [19] requires additional source of energy.

In previous papers [20-21], [22-23] authors design selective current harmonics observer, current controller, dc-link voltage control loop as well as mains voltage vector observer. All these control structures and observers are designed and investigated separately. The goal of this paper is to present results of the development and investigation of combined SAF control system which is based on the previous author's results [20], [21], [22], and [23].

2. PROBLEM STATEMENT

As it is shown in [24], according to Fortescue's theorem, consisted of N harmonics symmetrical load current $\mathbf{i}_L = (i_{Ld}, i_{Lq})^T$ in line voltage oriented reference frame (d-q) may be presented as:

$$i_{Ld} = \sum_{h=1}^{N} (x_{dph} + x_{dnh}),$$
$$i_{Lq} = \sum_{h=1}^{N} (x_{qph} + x_{qnh}), \qquad (1)$$

where $\mathbf{x}_h = (x_{dph}, x_{qph}, x_{dnh}, x_{qnh})^T$ – positive (p) and negative (n) sequences projections on d and q axes, h – harmonic number in (d-q) reference frame, $h=k-1$ for positive sequence, $h=k+1$ for negative sequence, k – harmonic number in (a-b) reference frame.

Note that 1st harmonic in (a-b) reference frame correspond to dc-signals (x_{d0}, x_{q0}) in (d-q) reference frame.

SAF is a voltage-source inverter with inductors L for filter currents i_A, i_B, i_C shaping by means of applied inverter voltages.

In **Ошибка! Источник ссылки не найден.** the following notations were used: u_A, u_B, u_C – mains phase voltages; $\mathbf{i_m}$ is mains currents vector; $\mathbf{i_{LABC}} = (i_{LA}, i_{LB}, i_{LC})^T$ – load currents; V_{dc} – dc-link voltage, R is equivalent filter and line resistance. Mains voltage vector observer provides information about grid voltage vector magnitude U_m, its angular position ε_0 and frequency ω_m.

Power filter averaged model is defined as [15]:

$$\dot{i}_A = (u_A - p_A V_{dc} - R i_A)/L,$$
$$\dot{i}_B = (u_B - p_B V_{dc} - R i_B)/L,$$
$$\dot{i}_C = (u_C - p_C V_{dc} - R i_C)/L, \qquad (2)$$
$$\dot{V}_{dc} = (i_A p_A + i_B p_B + i_C p_C)/C,$$

where: $dx/dt = \dot{x}$, $p_A, p_B, p_C \in [0,1]$ are control inputs for inverter; C – dc-link capacitance.

A system (2) can be presented in line voltage vector oriented reference frame (d-q) as

ISSN 2617-4316 (Print)
ISSN 2663-7723 (Online)

$$\dot{\mathbf{i}} = \begin{bmatrix} -\frac{R}{L} & \omega_m \\ -\omega_m & -\frac{R}{L} \end{bmatrix} \mathbf{i} - \frac{V_{dc}}{L}\mathbf{p}^* + \frac{1}{L}\begin{bmatrix} U_m \\ 0 \end{bmatrix}, \quad (3)$$
$$\dot{V}_{dc} = \frac{3}{2C}\left(i_d p_d + i_q p_q\right),$$

where: $\mathbf{i} = (i_d, i_q)^T$ – is a SAF current vector; $\mathbf{p}^* = \left(p_d, p_q\right)^T$ is a control vector.

The current balance for SAF is

$$\mathbf{i}_m = \mathbf{i}_L - \mathbf{i}, \quad (4)$$

where $\mathbf{i}_m = (i_{md}, i_{mq})^T$ is mains current vector.

The aim of the SAF is to compensate reactive current component x_{q0} together with higher order harmonics, such that mains current should contain only active current component x_{d0}. At the same time, dc-link voltage has to be kept in the admissible range for avoiding the SAF instability.

Assume that:

a) dc-link voltage V_{dc} , load current $\mathbf{i}_L$ and SAF currents $\mathbf{i}$ are available for measurements;

b) inductance $L > 0$ and $R > 0$ are known and constant;

The control objectives are defined as

$$\lim_{t\to\infty} i_d = x_{dph} + x_{dnh},$$
$$\lim_{t\to\infty} i_q = x_{q0} + x_{qph} + x_{qnh},, \quad (5)$$
$$\lim_{t\to\infty} \tilde{V}_{dc} < A,$$

where: $\tilde{V}_{dc} = V_{dc}^2 - V_{dc}^{*2}$ is voltage regulation error, $V_{dc}^* = const$ is dc-link voltage reference; A – voltage regulation errors admissible range.

3. LOAD CURRENT HARMONICS ESTIMATION

From (1) and (5) the current references are constructed as:

$$i_{dh}^* = \left(\hat{x}_{dph} + \hat{x}_{dnh}\right),$$
$$i_{qh}^* = i_{Lq} = \hat{x}_{q0} + \left(\hat{x}_{qph} + \hat{x}_{qnh}\right), \quad (6)$$

where: $\hat{x}_{q0}$ is estimate of x_{q0} and $\hat{x}_{dph}, \hat{x}_{dnh}, \hat{x}_{qph}, \hat{x}_{qnh}$ are estimates of $x_{dph}, x_{dnh}, x_{qph}, x_{qnh}$ obtained from the Luenberger observer [24], given by:

$$\dot{\hat{\mathbf{x}}} = \mathbf{A}_h\hat{\mathbf{x}} - \mathbf{K}_h\left[\mathbf{i}_L - \mathbf{C}_h\hat{\mathbf{x}}\right], \quad (7)$$

where: $\hat{\mathbf{x}} = (\hat{x}_{dph}, \hat{x}_{dnh}, \hat{x}_{qph}, \hat{x}_{qnh})^T$,

$$\mathbf{A}_h = \begin{pmatrix} 0 & -\omega_h & 0 & 0 \\ \omega_h & 0 & 0 & 0 \\ 0 & 0 & 0 & \omega_h \\ 0 & 0 & -\omega_h & 0 \end{pmatrix}, \mathbf{K}_h = \begin{pmatrix} -k_{1h} & -k_{2h} \\ k_{2h} & -k_{1h} \\ -k_{1h} & k_{2h} \\ -k_{2h} & -k_{1h} \end{pmatrix},$$

$\mathbf{C}_h[2,4] = \begin{bmatrix} 1 & 0 & 1 & 0 \\ 0 & 1 & 0 & 1 \end{bmatrix}$; k_h – observer gains; ω_h – harmonic angular frequency.

It is shown in [20] that equidistant to the imaginary axis poles arrangement ensures that the estimation of each harmonic attenuates with the same speed. Such observer tuning provides selectivity properties and high estimation convergence rate.

Having formed the given position of the observer poles as

$$\mathbf{P} = \begin{pmatrix} -r - j\omega_h \\ -r + j\omega_h \\ -r + j\omega_h \\ -r - j\omega_h \end{pmatrix}, \quad (8)$$

where *r* is the real part of complex number, $j = \sqrt{-1}$. The gains k_{1h}, k_{2h} of the observer matrix $\mathbf{K}_h$ are calculated in Matlab by the function *place()*.

Since observer (7) does not provide the estimation of direct current components, the active and reactive current components x_{d0} and x_{q0} are obtained from low pass filter

$$\dot{\hat{x}}_{d0} = -\tau_f^{-1}\hat{x}_{d0} + \tau_f^{-1} i_{Ld},$$
$$\dot{\hat{x}}_{q0} = -\tau_f^{-1}\hat{x}_{q0} + \tau_f^{-1} i_{Lq}, \quad (9)$$

where time constant τ_f is chosen to provide negligible values of higher order harmonics.

Note that derivatives of the estimated components $\dot{\hat{x}}_{dph}, \dot{\hat{x}}_{dnh}, \dot{\hat{x}}_{qph}, \dot{\hat{x}}_{qnh}$ and $\dot{\hat{x}}_{q0}$ are known functions.

4. CURRENT AND DC-LINK VOLTAGE CONTROL ALGORITHM

4.1. Current controller

In order to achieve harmonic compensation, the SAF output currents should be formed as the sum of the existing harmonic distortion components and reactive load current component with the opposite sign.

As it is shown in [21-22], one can apply feedback-linearizing controller for current regulation in the following form:

$$\mathbf{p}^* = \frac{1}{V_{dc}} \left\{ \begin{bmatrix} 0 & \omega_m L \\ -\omega_m L & 0 \end{bmatrix} \mathbf{i} + \begin{pmatrix} U_m \\ 0 \end{pmatrix} - \mathbf{v} \right\},\ V_{dc} > 0\ ,(10)$$

where $\mathbf{v} = (v_d, v_q)^T$ are control actions described as

$$\begin{aligned} v_d &= L\left(\frac{R}{L} i_d^* + \dot{i}_d^* - k_{i1}\tilde{i}_d + z_d\right),\ \ \dot{z}_d = -k_{ii}\tilde{i}_d, \\ v_q &= L\left(\frac{R}{L} i_q^* + \dot{i}_q^* - k_{i1}\tilde{i}_q + z_q\right),\ \ \dot{z}_q = -k_{ii}\tilde{i}_q. \end{aligned} \quad (11)$$

In (11) z_d, z_q are current controller integral terms, $k_{i1} > 0$, $k_{ii} > 0$ are proportional and integral gains of current controller, $\tilde{i}_d = i_d - i_d^*$, $\tilde{i}_q = i_q - i_q^*$ are current regulation errors, $\dot{i}_{dh}^*$, $\dot{i}_{qh}^*$ – derivatives of current references.

After substitution of (10), (11) in (3) we obtain the equation of currents error dynamics

$$\begin{aligned} \dot{z}_d &= -k_{ii}\tilde{i}_d, \\ \dot{\tilde{i}}_d &= -k_i\tilde{i}_d + z_d, \end{aligned} \quad (12)$$

$$\begin{aligned} \dot{z}_q &= -k_{ii}\tilde{i}_q, \\ \dot{\tilde{i}}_q &= -k_i\tilde{i}_q + z_q, \end{aligned} \quad (13)$$

where $k_i = R/L + k_{i1}$.

The resulting dynamics of each current loop is given by the linear 2nd order system (12), (13) which are asymptotically stable $\forall\ (k_{i1}, k_{ii}) > 0$, hence $\lim_{t\to\infty}(\tilde{i}_d, z_d) = 0$, $\lim_{t\to\infty}(\tilde{i}_q, z_q) = 0$. Since harmonics observer (7) is asymptotic, therefore for the mains currents we have $\lim_{t\to\infty} i_{md} = \lim_{t\to\infty}(i_{Ld} - i_d) = x_{d0}$, $\lim_{t\to\infty} i_{mq} = \lim_{t\to\infty}(i_{Lq} - i_q) = 0$, i.e. the control objectives of higher harmonics and reactive power compensation are achieved.

4.2. SAF dc-link voltage controller

For the stable SAF operation it is required to maintain the dc-link voltage V_{dc} in the permissible range, at the same time injecting the compensation current for harmonic distortions.

Taking into account (10), the voltage dynamics can be written as [23]

$$\dot{V}_{dc} = \frac{3}{2CV_{dc}}\left(i_d U_m - i_d v_d - i_q v_q\right). \quad (14)$$

The voltage regulation error dynamics under conditions $\lim_{t\to\infty}(\tilde{i}_d, z_d) = 0$, $\lim_{t\to\infty}(\tilde{i}_q, z_q) = 0$ is given by

$$\dot{\hat{V}}_{dc} = \frac{3}{C}\left(i_d^* U_m - i_d^* v_d - i_q^* v_q\right). \quad (15)$$

Define $i_d^* = i_{dh}^* + i_{dc}^*$ and $i_q^* = i_{qh}^*$, where i_{dc}^* is a reference for dc-link voltage stabilization current, and rewrite (11) and (15) as

$$\begin{aligned} v_d &= L\left(\frac{R}{L} i_{dh}^* + \frac{R}{L} i_{dc}^* + \dot{i}_{dh}^* + \dot{i}_{dc}^*\right), \\ v_q &= L\left(\frac{R}{L} i_{qh}^* + \dot{i}_{qh}^*\right), \end{aligned} \quad (16)$$

$$\begin{aligned} \dot{\hat{V}}_{dc} = \frac{3}{C}\Big(&\left(U_m - Ri_{dc}^*\right)i_{dc}^* - Li_{dc}^*\dot{i}_{dc}^* + U_m i_{dh}^* - 2Ri_{dc}^* i_{dh}^* - \\ &- Li_{dc}^*\dot{i}_{dh}^* - Li_{dh}^*\dot{i}_{dc}^* - Li_{dh}^*\dot{i}_{dh}^* - Li_{qh}^*\dot{i}_{qh}^* - \\ &- Ri_{dh}^{*2} - Ri_{qh}^{*2}\Big). \end{aligned} \quad (17)$$

In equation (17) the components $U_m i_{dh}^*$, $2Ri_{dc}^* i_{dh}^*$, $Li_{dc}^*\dot{i}_{dh}^*$, $Li_{dh}^*\dot{i}_{dc}^*$, $Li_{dh}^*\dot{i}_{dh}^*$, $Li_{qh}^*\dot{i}_{qh}^*$ have null average values for the period in quasi-steady state as far as $\mathbf{i}_h^*$ are sinusoidal signals. Components Ri_{dh}^{*2}, Ri_{qh}^{*2} have non-zero constant average values for a period, and therefore they need to be compensated by voltage controller action.

To simplify further development we rewrite (17) in compact form

$$\begin{aligned} \dot{\hat{V}}_{dc} = \frac{3}{C}\big((&U_m - Ri_{dc}^*)i_{dc}^* - Li_{dc}^*\dot{i}_{dc}^* + \\ &+ f_0(i_{dh}^*, i_{qh}^*) + f_n(i_{dh}^{*2}, i_{qh}^{*2})\big), \end{aligned} \quad (18)$$

where

$$\begin{aligned} f_0\left(i_{dh}^*, i_{qh}^*\right) &= U_m i_{dh}^* - 2Ri_{dc}^* i_{dh}^* - \\ &\quad - Li_{dc}^*\dot{i}_{dh}^* - Li_{dh}^*\dot{i}_{dc}^* - Li_{dh}^*\dot{i}_{dh}^* - Li_{qh}^*\dot{i}_{qh}^*, \\ f_n\left(i_{dh}^{*2}, i_{qh}^{*2}\right) &= -Ri_{dh}^{*2} - Ri_{qh}^{*2}. \end{aligned} \quad (19)$$

In (18) a reference current i_{dc}^* is the control action for nonlinear dc-link voltage dynamics. For partial linearization of (18) we apply the following nonlinear transformation

$$\eta = \left(U_m - Ri_{dc}^*\right)i_{dc}^*, \quad (20)$$

whose derivative is

$$\dot{\eta} = \left(U_m - 2Ri_{dc}^*\right)\dot{i}_{dc}^*. \quad (21)$$

Substituting (20) into (18), we obtain:

$$\dot{\hat{V}}_{dc} = \frac{3}{C}\left(\eta - Li_{dc}^*\dot{i}_{dc}^* + f_0\left(i_{dh}^*, i_{qh}^*\right) + f_n\left(i_{dh}^{*2}, i_{qh}^{*2}\right)\right). (22)$$

The desired dynamics of variable η can be constructed from (22) in the form of a PI-voltage controller with a low-pass filter:

$$\dot{\eta} = -\frac{1}{\tau_{dc}}\eta - \frac{k_v}{\tau_{dc}}\tilde{V}_{dc} + \frac{1}{\tau_{dc}}x_v, \quad \dot{x}_v = -k_{vi}\tilde{V}_{dc}, \tag{23}$$

where: $k_v > 0$, $k_{vi} > 0$ are proportional and integral gains of voltage controller; x_v – voltage controller integral term; τ_{dc} – filter time constant.

The linearized dynamics of (22) and (23) with $Li_{dc}^{*}\dot{i}_{dc}^{*} + f_0\left(i_{dh}^{*}, i_{qh}^{*}\right) + f_n\left(i_{dh}^{*2}, i_{qh}^{*2}\right) = 0$ is a linear third-order system which always can be designed as asymptotically stable by proper selection of the three tuning parameters k_v, k_{vi} and τ_{dc}.

To obtain desired dynamics of (23), the equation (21) is solved for $\dot{i}_{dc}^{*}$ in the following form:

$$\dot{i}_{dc}^{*} = -\frac{1}{\tau_{dc}}\frac{1}{U_m - 2Ri_{dc}^{*}}\left(\eta - k_v\tilde{V}_{dc} + x_v\right), \quad \dot{x}_v = -k_{vi}\tilde{V}_{dc}. \tag{24}$$

From (24) and (20) it follows that internal nonlinear dynamics of i_{dc}^{*} is stable provided that $\left(U_m - 2Ri_{dc}^{*}\right) > 0$.

Nonlinear dynamic voltage controller (24) guarantees: a) partial linearization of (18); b) integral term x_v provides compensation for constant average value of $f_n\left(i_{dh}^{*2}, i_{qh}^{*2}\right)$; c) information about derivative $\dot{i}_{dc}^{*}$ needed for d-current controller (16).

If filter time constant τ_{dc} is selected small enough, then quasi-steady state solution of (23) is

$$\eta = -k_v\tilde{V}_{dc} + x_v, \quad \dot{x}_v = -k_{vi}\tilde{V}_{dc}, \tag{25}$$

and reduced second-order system (22), (25) with $Li_{dc}^{*}\dot{i}_{dc}^{*} + f_0\left(i_{dh}^{*}, i_{qh}^{*}\right) + f_n\left(i_{dh}^{*2}, i_{qh}^{*2}\right) = 0$ is asymptotically stable $\forall \ \left(k_v, k_{vi}\right) > 0$.

Tuning of the closed-loop system (22), (23) by selection of the four parameters (C, k_v, k_{vi} and τ_{dc}) should provide the acceptable voltage regulation dynamics together with filtering of the high frequency harmonic perturbations, generated by $f_0\left(i_{dh}^{*}, i_{qh}^{*}\right)$, $f_n\left(i_{dh}^{*2}, i_{qh}^{*2}\right)$ terms.

5. MAINS VOLTAGE VECTOR OBSERVER DESIGN

For the practical implementation of developed SAF control system, the information about line grid voltage vector magnitude U_m, angular position ε_0 and frequency ω_m is required. Generally U_m and ω_m are not constant parameters and can be slowly varying in time. In order to overcome this problem and reduce influence of measurement noise we propose to use the voltage observer, designed in this Section, which is adaptive to unknown angular frequency ω_m.

The vector of grid voltage in (a-b) reference frame is defined by

$$\begin{pmatrix} u_{ma} \\ u_{mb} \end{pmatrix} = \begin{pmatrix} U_m\cos\left(\varepsilon_0\right) \\ U_m\sin\left(\varepsilon_0\right) \end{pmatrix}, \ \dot{\varepsilon}_0 = \omega_m. \tag{26}$$

Assume that voltage vector components u_{ma} and u_{mb} are available for measurement, ω_m is unknown parameter, $\left(u_{ma}, u_{mb}, \omega_m\right)$ are bounded. Under these assumptions it is necessary to design adaptive observer which guarantees

$$\lim_{t\to\infty}\left(\tilde{u}_{ma}, \tilde{u}_{mb}, \tilde{\omega}_m\right) = 0, \tag{27}$$

where: $\tilde{u}_{ma} = u_{ma} - \hat{u}_{ma}$; $\tilde{u}_{mb} = u_{mb} - \hat{u}_{mb}$; $\tilde{\omega}_m = \omega_m - \hat{\omega}_m$ are the estimation errors; $\hat{u}_{ma}$, $\hat{u}_{mb}$, $\hat{\omega}_m$ – estimates of u_{ma}, u_{mb} and ω_m correspondingly.

The signals (26) may be presented as a solutions of the following dynamic system:

$$\dot{u}_{ma} = -\omega_m u_{mb}, \ u_{ma}(0) = U_m, \quad \dot{u}_{mb} = \omega_m u_{ma}. \tag{28}$$

For dynamic system (28) we design the following adaptive observer

$$\begin{aligned} \dot{\hat{u}}_{ma} &= -\hat{\omega}_m u_{mb} + k_u\tilde{u}_{ma}, \\ \dot{\hat{u}}_{mb} &= \hat{\omega}_m u_{ma} + k_u\tilde{u}_{mb}, \\ \dot{\hat{\omega}}_m &= -\gamma_u\left(\tilde{u}_{ma}u_{mb} - \tilde{u}_{mb}u_{ma}\right), \end{aligned} \tag{29}$$

where: k_u and γ_u are the tuning gains.

According to (28) and (29) estimation the errors dynamics becomes

$$\begin{aligned} \dot{\tilde{u}}_{ma} &= -\tilde{\omega}_m u_{mb} - k_u\tilde{u}_{ma}, \\ \dot{\tilde{u}}_{mb} &= \tilde{\omega}_m u_{ma} - k_u\tilde{u}_{mb}, \\ \dot{\tilde{\omega}}_m &= \gamma_u\left(\tilde{u}_{ma}u_{mb} - \tilde{u}_{mb}u_{ma}\right). \end{aligned} \tag{30}$$

For stability proof of the system (30) let us consider the following positive-definite Lyapunov`s function

$$V = \frac{1}{2}\left(\tilde{u}_{ma}^2 + \tilde{u}_{mb}^2 + \gamma_u^{-1}\tilde{\omega}_m^2\right). \qquad (31)$$

The total derivative of (31) along the trajectories of (30) is

$$\dot{V} = -k_u\left(\tilde{u}_{ma}^2 + \tilde{u}_{mb}^2\right). \qquad (32)$$

Hence, the positive-definite V, given by (31), is a Lyapunov function.

From (31) and (32) it follows that $\left(\tilde{u}_{ma}, \tilde{u}_{mb}, \tilde{\omega}_m\right)$ are bounded. Therefore for bounded $\left(u_{ma}, u_{mb}, \omega_m\right)$ estimates $\left(\hat{u}_{ma}, \hat{u}_{mb}, \hat{\omega}_m\right)$ are bounded as well. Furthermore, derivatives $\left(\dot{\tilde{u}}_{ma}, \dot{\tilde{u}}_{mb}\right)$ are also bounded.

Due to $\int_0^t \dot{V} d\tau = -\left[V(t) - V(0)\right]/k_u \le V(0)/k_u$, $\tilde{u}_{ma}(t), \tilde{u}_{mb}(t)$ are square-integrable, and have bounded derivatives. Applying the Barbalat's Lemma [25], we have $\lim_{t\to\infty}\tilde{u}_{ma} = 0$, $\lim_{t\to\infty}\tilde{u}_{mb} = 0$.

System (30) can be presented in the following standard form:

$$\begin{aligned} \dot{\tilde{\mathbf{u}}}_m &= \mathbf{A}_u\tilde{\mathbf{u}}_m + \mathbf{\Gamma}_u(t)\tilde{\omega}_m, \\ \dot{\tilde{\omega}}_m &= -\gamma_u\mathbf{\Gamma}_u(t)\tilde{\mathbf{u}}_m, \end{aligned} \qquad (33)$$

where: $\tilde{\mathbf{u}}_m = \left(\tilde{u}_{ma}, \tilde{u}_{mb}\right)^T$; $\mathbf{\Gamma}_u = \left(-u_{ma}, u_{mb}\right)$; $\mathbf{A}_u$ is a Hurwitz matrix.

The persistency of excitation conditions for system (33) are:

$$\int_t^{t+T} \mathbf{\Gamma}_u(\tau)\mathbf{\Gamma}_u^T(\tau)d\tau > 0,\ T > 0,\ \forall t \ge 0. \qquad (34)$$

Since $\mathbf{\Gamma}_u(t), \dot{\mathbf{\Gamma}}_u(t)$ are bounded, an equilibrium $\left(\tilde{u}_{ma}, \tilde{u}_{mb}, \tilde{\omega}_m\right) = 0$ of (30) is globally exponentially stable [25]. Therefore, objective (27) of asymptotic estimation are achieved. Condition (34) is equivalent to $\left(u_{ma}^2 + u_{mb}^2\right) > 0$, i.e. voltage vector magnitude should not be zero.

Coordinate transformations between (a-b) and (d-q) reference frames is performed using

$$cos\left(\varepsilon_0\right) = \frac{\hat{u}_{ma}}{\hat{U}_m},\ sin\left(\varepsilon_0\right) = \frac{\hat{u}_{mb}}{\hat{U}_m},\ \hat{U}_m = \sqrt{\hat{u}_{ma}^2 + \hat{u}_{mb}^2}.$$

6. SIMULATION RESULTS AND EXPERIMENTAL STUDY

6.1. Test conditions

Harmonic observer (7) and adaptive line voltage observer (29) are implemented on floating-point 32-bit DSP TMS320F28335 and verified experimentally, while complete SAF dynamics has been investigated by simulations.

During experiment line grid voltage with magnitude $U_m = 230$ V and angular frequency $\omega_m = 314$ rad/s as well as phase currents are measured by Hall-effect sensors. Non-linear load is represented by a bridge rectifier with capacitance dc-link filter and chopper for load current regulation. Sampling time during experiments is set to T_s = 75 μs.

SAF parameters are: $R = 0.12$ Ohm, $L = 3$ mH, $C = 1000$ μF, and dc-link reference voltage $V_{dc}^* = 700$ V. Initial dc-link voltage is $V_{dc}(0) = 540$ V. Current controllers gains are selected as $k_{i1} = 800$, $k_{ii} = 320000$, voltage controller gains are $k_v = 0.03$, $k_{vi} = 0.8$, and time constant of the dc-link voltage controller filter is set as $\tau_{dc} = 5\cdot10^{-4}$ s, $\tau_f = 0.1$s. Tuning coefficients and initial conditions for voltage observer were set to $k_u = 850$, $\gamma_u = 4$, $\hat{u}_{ma}(0) = 0$, $\hat{u}_{mb}(0) = 0$, $\hat{\omega}_m(0) = 0$.

6.2. Mains voltage observer performance

Experimental transients of line voltage vector estimation are shown in Fig. 2. As it follows from Fig. 2, the proposed adaptive observer provide fast asymptotic estimation of u_{ma}, u_{mb} and ω_m. Convergence time is approximately 0.012 s, which is smaller than period of line grid voltage.

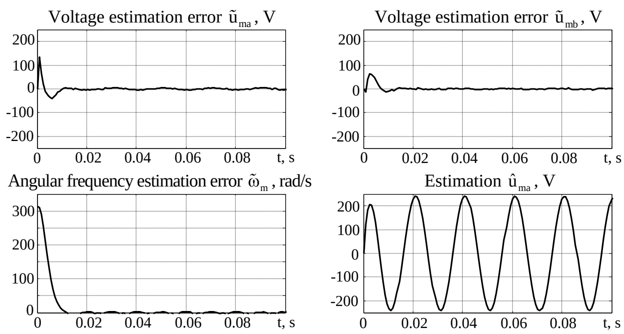

Fig. 2. **Transients during estimation of u_{ma}, u_{mb} and ω_m**
***Source*: compiled by the author**

6.3. SAF control system performance

Standalone harmonic observer (7) was tuned for estimation of harmonics with order 5, 7, 11, 13, 17, 19 and verified by simulations and experimentally in real-time. It is established, that simulation results under recorded experimental data are the same with experimental results in real-time. Due to this fact, complete SAF dynamics has been investigated by simulations using recorded arrays of experimental data. The initial time interval is given to establish the dc-link voltage, at time $t = 0.6$ s starts estimation of reactive current, at time $t = 1$ s SAF is activated to estimate harmonics and compensate reactive power and harmonic distortions. Transients for this test are shown in Fig. 3.

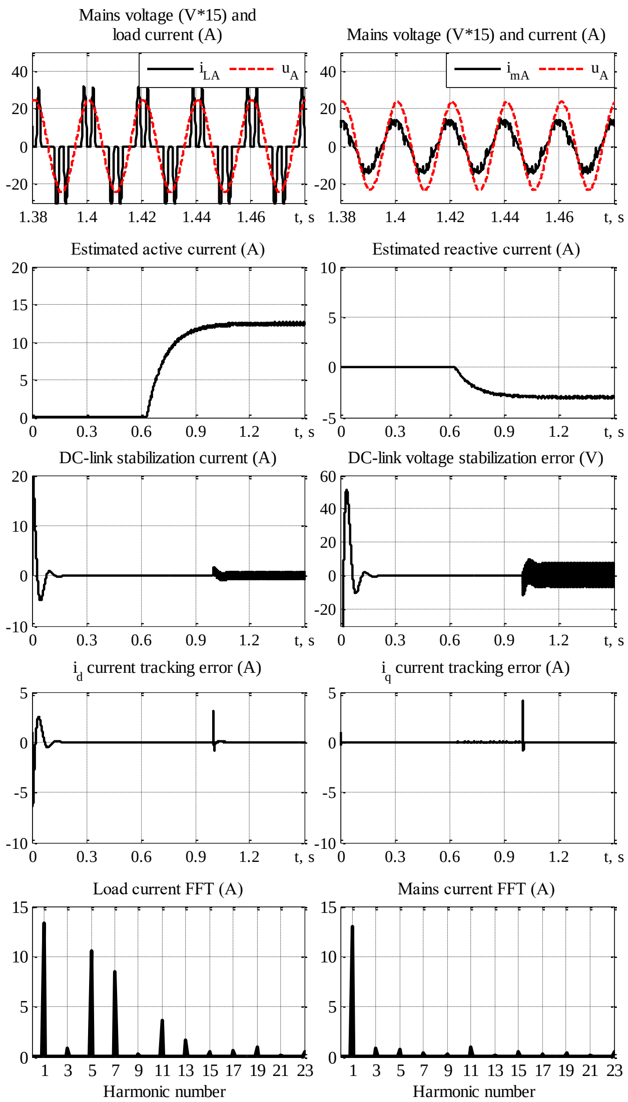

Fig. 3. **The transients of SAF operation**

***Source*: compiled by the author**

From the analysis of the mains voltages and currents, load currents and their FFT characteristics presented in Fig. 3, it follows that harmonic distortions in mains current with order 5, 7, 11, 13, 17 and 19 are significantly decreased due to SAF operation. Other harmonics, existing in the load current spectrum are not compensated and have the same magnitude in mains current spectrum. Despite the presence of these uncompensated harmonics, mains current waveform is very close to the sinusoidal shape. Phase shift between mains voltage and current is close to zero, hence compensation of reactive power is also achieved. From the current tracking errors transients it can be concluded that asymptotic current regulation is achieved. From dc-link stabilization error dynamics one can found out those high frequency components in dc-link voltage are small enough and correspond to acceptable range.

CONCLUSIONS

Complete SAF control system is designed and experimentally verified. Harmonics observer is tuned according to simplified approach and provides fast selective asymptotic estimation of the load current. The proposed tuning approach greatly simplifies technical implementation of the SAF due to reducing requirements for the computing performance of the controller and power electronics quality.

Harmonics observer generates the compensation current reference for the current controller, which provide asymptotic current tracking.

Nonlinear dc-link voltage controller guarantees asymptotic average voltage regulation and allows to keep the dc-link voltage in admissible range. Reconstruction of the current reference derivative results in full decoupling of current control loop and dc-link voltage control loop so dc-link stabilization current do not influence on the harmonics compensation process.

Adaptive observer of the line voltage vector provides information about its magnitude, angular position and frequency.

Effectiveness of the designed system is proved by simulations and experiments.

REFERENCES

1. "IEEE Recommended Practice and Requirements for Harmonic Control in Electric Power Systems". *IEEE Std 519-2014 Revis. IEEE Std 519-1992*, p. 1–29.
2. Motta L. & Faúndes N. "Active / passive harmonic filters: Applications, challenges trends". In *2016 17th International Conference on Harmonics and Quality of Power (ICHQP)*. Oct. 2016. p.657–662. DOI: 10.1109/ICHQP.2016.7783319.
3. Kazem H. A. "Harmonic mitigation techniques applied to power distribution networks". *Advances in Power Electronics*. 2013. p. 1–10.
4. Morán, L. Dixon, J. & Torres, M. "41 – Active Power Filters". In *Power Electronics Handbook (Fourth Edition)*. M. H. Rashid, Ed. Butterworth-Heinemann. 2018. p. 1341–1379.
5. Dugan, R. C. Santoso, S. McGranaghan, M. F. & Beaty, H. W. "Electrical Power Systems Quality". New York: McGraw Hill Professional. 2002. 546 p.
6. Akagi, H. Watanabe E. H. & Aredes, M. "Instantaneous Power Theory and Applications to Power Conditioning". New Jersey: John Wiley & Sons. 2007. 396 p.
7. F. C. D. L. Rosa. "Harmonics and Power Systems". Boca Raton: *CRC Press*. 2006. 216 p.
8. Tilli, A. Ronchi, F. & Tonielli, A."Shunt active filters: selective compensation of current harmonics via state observer". *IEEE 2002 28th Annual Conference of the Industrial Electronics Society. IECON 02*. 2002; Vol.2: 874–879.
9. M. S. A. Dahidah, Konstantinou, G. & Agelidis, V. G. "A Review of Multilevel Selective Harmonic Elimination PWM: Formulations, Solving Algorithms, Implementation and Applications". *IEEE Trans. Power Electron.* Aug. 2015; Vol. 30 No. 8: 4091–4106. DOI: 10.1109/TPEL.2014.2355226.
10. Kumar, D. & Zare, F. "Harmonic analysis of grid connected power electronic systems in low voltage distribution networks". *IEEE Journal of Emerging and Selected Topics in Power Electronics*. 2016; Vol.4 No. 4: 70–79,
11. Wang, Y., Yong, J., Sun, Y., Xu, W. & Wong, D. "Characteristics of harmonic distortions in residential distribution systems". *IEEE Transactions on Power Delivery*. 2017; Vol. 32 No. 3: 1495–1504.
12. ABB DRIVES. "Technical guide No. 6 Guide to harmonics with AC drives. 3AFE64292714 REV F EN 27.11.2017 *20434". 32 p.
13. Liu, K., Cao, W., Zhao, J., You J. & Gu, Q. "Optimized current control and dynamic coordination strategy for large-capacity harmonic compensation system". *2016 IEEE 2nd Annual Southern Power Electronics Conference (SPEC)*. Auckland: 2016. p. 1–4.
14. Panda, G., Dash, S. K. & Sahoo, N. "Comparative performance analysis of Shunt Active power filter and Hybrid Active Power Filter using FPGA-based hysteresis current controller". In *2012 IEEE 5th India International Conference on Power Electronics (IICPE)*. Dec. 2012. p. 1–6. DOI: 10.1109/IICPE.2012.6450517.
15. Bacon, V. D. & S. A. O. da Silva. "Selective harmonic currents suppressing applied to a three-phase shunt active power filter based on adaptive filters". *2015 IEEE 13th Brazilian Power Electronics Conference and 1st Southern Power Electronics Conference (COBEP/SPEC)*. Fortaleza: 2015. p. 1–6.
16. Lascu, C., Asiminoaei, L., Boldea, I. & Blaabjerg, F. "High Performance Current Controller for Selective Harmonic Compensation in Active Power Filters". *IEEE Trans. Power Electron.* Sep. 2007; Vol. 22 No. 5: 1826–1835. DOI: 10.1109/TPEL.2007.904060.
17. He, J. & Liang, Beihua. "Selective harmonic compensation using active power filter with enhanced double-loop controller". *2016 IEEE 8th International Power Electronics and Motion Control Conference (IPEMC-ECCE Asia)*. Hefei: 2016. p. 2714–2718.
18. Tilli, A., Marconi, L. & Conficoni C. "Analysis, dimensioning and robust control of shunt active filter for harmonic currents compensation in electrical mains". *Recent Advances in Robust Control – Theory and Applications in Robotics and Electromechanics*, IntechOpen. 2011. p. 1–26.
19. Preetha, P. K., Surya, Babu S. & Manjula, G. Nair. "DC link voltage regulation in active filter using drainage power from distribution transformer". *2016 IEEE 1st International Conference on Power Electronics, Intelligent Control and Energy Systems (ICPEICES)*. Delhi: 2016. p. 1–4.

 ISSN 2617-4316 (Print)
ISSN 2663-7723 (Online)

20. Peresada, S., Zaichenko, Y. & Dymko, S.”Selective Estimation of Three-Phase Mains Current for Shunt Active Power Filter”. *2020 IEEE 7th International Conference on Energy Smart Systems (ESS)*. Kyiv: Ukraine 2020. p. 68–72. DOI: 10.1109/ESS50319.2020.9160201.

21. Peresada, S., Zaichenko, Y., Pushnitsyn, D. & Reshetnyk, V. “Adaptive current control for shunt active power filters under resistance and inductance uncertainty”. *IEEE International Conference on Intelligent Energy and Power Systems.* Kharkiv: 2018. p. 280–285.

22. Peresada, S., Kovbasa, S., Zaichenko, Y. & Reshetnyk, V. “Selective compensation of three-phase current harmonics”. *Technical Electrodynamics* (in Ukrainian). 2018; Vol. 4: 102–105.

23. Peresada, S., Zaichenko, Y. & Nikonenko, Y. “Partially Feedback Linearizing DC-Link Voltage Controller for Three-Phase Shunt Active Power Filters”. *2019 IEEE International Conference on Modern Electrical and Energy Systems (MEES).* Kremenchuk: Ukraine. 2019. p. 306–309.

24. Ronchi, F. & Tilli, A. “Three-phase positive and negative sequences estimator to generate current reference for selective active filters”. *IEEE Mediterranean conference on control and automation. MED2002.* Lisbon: 2002.

25. Narendra, K. & Annaswamy, A. “Stable Adaptive Systems“. New Jersey: Englewood Cliffs: Prentice Hall. 1989.

Conflicts of Interest: the authors declare no conflict of interest

Received 18.01.2021
Received after revision 23.02.2021
Accepted 11.03. 2021

DOI: 10.15276/aait.01.2021.4
УДК 621.314.5

ДИНАМІЧНА ПОВЕДІНКА СИСТЕМИ КЕРУВАННЯ СИЛОВИМ АКТИВНИМ ФІЛЬТРОМ

Сергій Михайлович Пересада[1]
ORCID: 0000-0001-8948-722X; sergei.peresada@gmail.com
Сергій Миколайович Ковбаса[1]
ORCID: 0000-0002-2954-455X; skovbasa@ukr.net
Юрій Михайлович Зайченко[1]
ORCID: 0000-0002-2933-7737; zaychenko_yura@i.ua
[1] Національний технічний університет України «Київський політехнічний інститут імені Ігоря Сікорського», просп. Перемоги, 37, Київ, Україна

АНОТАЦІЯ

Гармонічні спотворення в електричних мережах є добре відомими та достатньо вивченими явищами. Силовий активний фільтр визнано ефективним засобом для задоволення вимог нормативних документів, що регулюють якість електроенергії. Незважаючи на цей факт, їхня практична реалізація досі пов’язана зі значними складностями. Зокрема, в існуючих системах для оцінювання гармонічного складу струму мережі, як правило, використовуються методи на основі швидкого перетворення Фур’є або методи на основі теорії миттєвої потужності. Проте використання швидкого перетворення Фур’є вимагає високої обчислювальної здатності системи керування з однієї сторони, а застосування теорії миттєвої потужності значно підвищує вимоги до силової частини активного фільтра. Застосування іншого підходу – селективної компенсації гармонік, дає можливість зменшити вимоги до обчислювальної потужності та значно спростити технічну реалізацію активного фільтра і при цьому досягти прийнятного рівня компенсації спотворень. В статті представлено результати розробки та дослідження системи керування силовим активним фільтром. Запропонована система керування складається із селективного спостерігача гармонік, лінеаризуючого зворотним зв’язком регулятора струмів, регулятора напруги ланки постійного струму фільтра та спостерігача напруги мережі. Спостерігач гармонік, який налаштовано відповідно до спрощеної процедури, забезпечує селективне виявлення вищих гармонік струму мережі та формує завдання на струм компенсації, яке відпрацьовується регуляторами струмів. Нелінійний регулятор напруги забезпечує асимптотичне регулювання середнього значення напруги ланки постійного струму САФ, розв’язане з процесом компенсації струмів. Адаптивний спостерігач напруги мережі надає інформацію про амплітуду, частоту обертання та положення вектора напруги мережі. Запропоновану систему керування реалізовано на цифровому сигнальному процесорі TMS320F28335 та досліджено експериментально. Результати експериментальних досліджень разом із результатами моделювання підтверджують ефективність запропонованого рішення. Розроблена система керування може бути використаною для створення силових активних фільтрів.

Ключові слова: силовий активний фільтр; регулятор напруги ланки постійного струму; гармонічні спотворення; селективна компенсація гармонік

ABOUT THE AUTHORS

Sergiy Mykchailovych Peresada – Dr. Sci. (Eng) (2007), PhD (Eng) (1983), Professor, Head of the Automation of Electromechanical Systems and the Electrical Drives Department, National Technical University of Ukraine “Igor Sikorsky Kyiv Polytechnic Institute”, 37, Peremogy Ave., Kyiv, Ukraine
ORCID: 0000-0001-8948-722X; sergei.peresada@gmail.com
***Research field*:** Nonlinear Control of Multidimensional Electromechanical Systems With Partially Measured State Vector; Adaptive Control of Electromechanical Systems With AC Electric Motors

Сергій Михайлович Пересада – доктор технічних наук (2007), кандидат технічних наук (1983), професор, завідувач кафедри автоматизації електромеханічних систем та електроприводу Національного технічного університету України «Київський політехнічний інститут імені Ігоря Сікорського», просп. Перемоги, 37, Київ, Україна

Sergiy Mykolaiovych Kovbasa – Dr. Sci. (Eng) (2020), PhD (Eng) (2004), Associate Professor of the department automation of electromechanical systems and the electrical drives, National Technical University of Ukraine “Igor Sikorsky Kyiv Polytechnic Institute”, 37, Peremogy Ave., Kyiv, Ukraine
ORCID: 0000-0002-2954-455X; skovbasa@ukr.net
***Research field*:** AC Motors Nonlinear Control Systems; Semiconductor Converters Control; DSP Based Control Systems

Сергій Миколайович Ковбаса – доктор технічних наук (2020), кандидат технічних наук (2004), доцент кафедри автоматизації електромеханічних систем та електроприводу Національного технічного університету України «Київський політехнічний інститут імені Ігоря Сікорського», просп. Перемоги, 37, Київ, Україна

Yuriy Mykchailovych Zaichenko – PhD (Eng) (2020), Research Assistant of the department automation of the department automation of electromechanical systems and the electrical drives, National Technical University of Ukraine “Igor Sikorsky Kyiv Polytechnic Institute”, 37, Peremogy Ave., Kyiv, Ukraine
ORCID: 0000-0002-2933-7737; zaychenko_yura@i.ua
***Research field*:** Semiconductor Converters Control; DSP Based Control Systems

Юрій Михайлович Зайченко – кандидат технічних наук (2020), асистент кафедри автоматизації електромеханічних систем та електроприводу Національного технічного університету України «Київський політехнічний інститут імені Ігоря Сікорського», просп. Перемоги, 37, Київ, Україна